Vol. A39 (1971) ACTA PHYSICA POLONICA Fasc. 1

THE TEMPERATURE DEPENDENCE OF THE MAGNETIZATION OF A SINGLE-DOMAIN PARTICLE ASSEMBLY

By J. Mizia, H. Figiel and K. Krop

Physics Department, Metallurgy Institute, Academy of Mining and Metallurgy, Cracow*

(Received April 6, 1970)

The magnetization of uniaxial single-domain particles in thermal equilibrium with their surroundings is predicted theoretically. In particular, the demagnetization curves, time variations of magnetization and coercive force are found for a randomly oriented assembly of particles with different volume-to-temperature ratios. The mean energy barrier for these particles is also estimated.

Introduction

We assume here that the magnetic particles are located in a non-magnetic matrix and their volume density is low enough for their magnetostatic interaction to be negligible. Moreover, we assume that the particles have uniaxial magnetic anisotropy of constant $K_u > 0$.

Stoner and Wohlfarth (1948), hereafter referred to as SW, evaluated the coherent rotation of the magnetization vector of a unixial single-domain particle (with $K_u > 0$) under the effect of an applied field.

Nèel (1949) proved that thermal agitation causes the lifetime of the minimum energy state to become finite, this being expressed by

$$\tau = \tau_0 \exp (E/kT) \tag{1}$$

where E is the energy barrier. Following Bean and Livingston (1959) it is assumed that τ_0 is independent of external field (H) and the particle's volume (V), and that $\tau_0 \simeq 10^{-11}$ sec. This simplified model is valid for $E = K_u V \gg kT$ (for $K_u V \gg 10\,kT$ one obtains $a_1 = 25\, kT/2K_u V \leqslant 1.25$).

Following the method proposed by Gaunt (1968), the influence of thermal agitation on SW rotation for $K_u V \gg kT$ ($a_1 \leqslant 1.25$) is analyzed in this paper.

---

* Address: Zakład Fizyki, Instytut Metalurgii, Akademia Górniczo-Hutnicza, Kraków, Al. Mickiewicza 30, Poland.

Particles with anisotropy axis parallel to external field

In the case of a particle with anisotropy axis parallel to field H the angle θ in Fig. 1 is equal to zero. For the variable part of the magnetic free energy we then have

$$E_S = K_u V \sin^2 \varphi - I_S VH \cos \varphi \tag{2}$$

where φ is the angle between the direction of the particle's moment and the positive direction of the magnetic field H. H is positive in the direction of the saturating field.

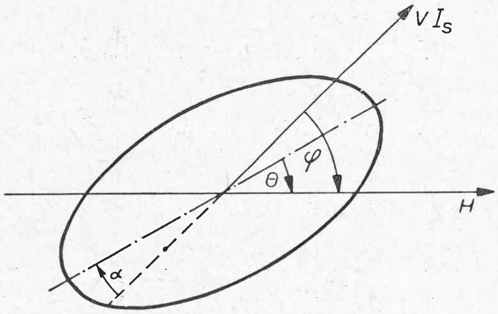

Fig. 1. Particle with uniaxial anisotropy (easy axis = ellipsoid axis) in external magnetic field

It is possible to calculate the energy barrier from Eq. (2):

$$E = E_S^{\max} - E_S^{\min} = K_u V (1+h)^2 \tag{3}$$

where $h = HI_S/2K_u$, I_S being the saturation magnetization of a cobalt particle.

Figure 2 depicts the energy barriers $E_{i,k}$ for the transition of the particle's moment from orientation i to orientation $j (i = 1,2$ and $j = 1,2$, where 1 denotes the φ_1 state and 2 the φ_2

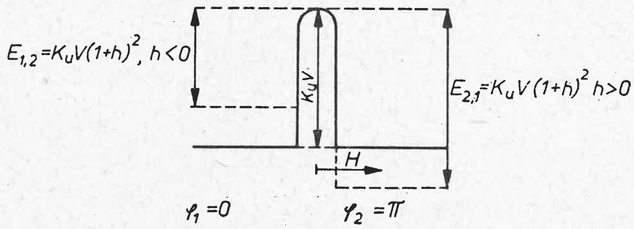

Fig. 2. Dependence of energy of uniaxially anisotropic particle on the angle between the magnetic moment and a field H applied along the easy axis sensed oppositely to the saturating field (and at the same to the magnetic moment of the particle)

state). φ_1 and φ_2 in Fig. 2 are the angles relative to the positive direction of the field. The sign of h is positive or negative accordingly for the magnetic moment parallel or antiparallel to the field H.

Owing to the thermal agitation there is a certain probability that the particle's moment will jump from the i orientation to the j orientation within time dt. If in the state 1 there are

n_1 particles, and in the state 2 -- n_2 particles, we can write the equation

$$\frac{dn_1}{dt} = -\frac{dn_2}{dt} = \tau_{2,1}^{-1} n_2 - \tau_{1,2}^{-1} n_1. \tag{4}$$

It follows from Eq. (4) that with the initial condition $n_1 = n_2$ we have

$$n(t) = n_2 - n_1 = n_S[1 - \exp(-t/\tau)] \tag{5}$$

where

$$n_S = \frac{\tau_{2,1} - \tau_{1,2}}{\tau_{2,1} + \tau_{1,2}} n, \ \tau^{-1} = \tau_{1,2}^{-1} + \tau_{2,1}^{-1} \text{ and } n = n_1 + n_2$$

for the states 1 and 2. Putting the dependence (1) into relation (3) we have

$$\tau_{2,1}/\tau_{1,2} = \exp\left(\frac{2I_S H}{kT} V\right). \tag{6}$$

If we assume $\tau_{2,1}/\tau_{1,2} \gg 1$, what means that

$$\frac{2I_S H}{kT} V \geqslant 5 \text{ to } 10,$$

we get

$$\tau \simeq \tau_{1,2} \text{ and } n_S \simeq n.$$

The above assumption which simplifies calculations is applied throughout the paper when two energy minima are asymmetrized by the application of an external field H.

The given field H is a coercive field (H_c) if the time of its application $t = \tau \simeq \tau_{1,2}$. This leads to the relation

$$t = \tau_0[K_u V(1-|h_0|)^2/kT] \tag{7}$$

whence

$$K_u V(1-|h_c|^2) = kT(\ln t + 25)$$

where t is time counted in seconds, and

$$|h_c| = 1 - \sqrt{2a}, \text{ where } a = \frac{25kT}{2K_u V}\left(1 + \frac{\ln t}{25}\right) \tag{8}$$

what for $t = 1$ sec gives the formula derived by Bean and Livingston (1959):

$$H_c = \frac{2K_u}{I_S}\left[1 - 5\left(\frac{kT}{K_u V}\right)^{1/2}\right]. \tag{9}$$

Expansion of Gaunt's method

The considerations above are possible analytically only for $\theta = 0$. Gaunt (1968) derived a numerical technique of solving the problem for any θ. Commencing with the equation

$$E_S = K_u V \sin^2(\varphi - \theta) - HI_S V \cos \varphi \tag{10}$$

and defining the reduced energy, $\eta = E_S/2K_uV$, we have from the minimum energy condition

$$\eta' = \frac{d\eta}{d\varphi} = \frac{1}{2}\sin 2(\varphi-\theta) + h\sin\varphi = 0. \tag{11}$$

This equation can be used for determining φ numerically for given values of h and θ. When $h > 1$ the reduced energy η takes on only a single minimum value at the value of $\varphi = \varphi_1$. Otherwise there may appear in addition a second minimum at $\varphi = \varphi_2$, a lower maximum at $\varphi = \varphi_m$ and a higher maximum which is of no interest to us. The graphical interpretation of φ as the angle between the direction of h and the tangent to the asteroid is well known (Oquey 1960). In this interpretation φ_1 is determined by the tangent to the left corner, φ_2 by the tangent to the right corner, and φ_m by the tangent to the lower corner of the asteroid (with oppositely directed magnetization vector).

Gaunt's reduced energy barrier is given by

$$\Delta\eta(\theta, h) = \eta(\varphi_m) - \eta(\varphi_1) \tag{12}$$

where φ_1 is the minimum in which the magnetic moment of the particle will be found at the reduction of field from $+\infty$ to the given value H.

The table given by Gaunt (1968) contains the above values of $\Delta\eta$ for several θ and $h(h < 0)$. It is terminated at $\theta = 45°$, for $\Delta\eta(\theta) = \Delta\eta\ (90°-\theta)$.

Thermal agitation is taken into account by assuming that the transition from state φ_1 to state φ_2 occurs among the particles of different angles θ relative to fild when the generalized Gaunt condition is satisfield, that is,

$$t = \tau(\theta_b, h) = \tau_0 \exp\left[\frac{2K_uV}{kT}\Delta\eta(\theta_b, h)\right] \tag{13}$$

what gives

$$\Delta\eta(\theta_b, h) = \frac{25\,kT}{2K_uV}\left(1 + \frac{\ln t}{25}\right) = a \tag{14}$$

where t is the time of action of field h, in sec, and θ_b is the angle θ for which Eq. (14) is satisfied.

Analyzing condition (13) shows that the following assumptions are concealed in it: 1) as before, the condition $\tau = \tau_{1,2}$ is accepted, *i. e.*, it is assumed that $\tau_{2,1}/\tau_{1,2} \gg 1$; 2) the boundaries of transitions are sharp, *i. e.* we assume that the jump occurs in time $t = \tau$; 3) it is assumed that thermal agitation affects the behaviour of the moments by diverting them from minimum φ_1 to φ_2, but the moments are either all in φ_1 or all in φ_2. This reasoning is true only approximately, when $K_uV \gg kT$ (for $K_u\ V \gg 10\ kT$ the straight line $a_1 = \frac{25kT}{2K_uV} \leqslant 1.25$ in Fig. 3 is obtained), for then the probability of intermediate states φ is relatively low owing to the large exponential factor. The assumptions 1) and 2) will be discussed later on.

(h, a) plane

Let us assume an isotropic distribution of the particles' easy axes (angles θ) in space. For a given (negative) h, those moments of particles will be reversed from the φ_1 state to the φ_2 state which have a θ-angle between θ_b and $90°-\theta_b$, where θ_b is identical for different a_1 and t giving the same a in Eq. (14). The relative magnetization I/I_S of such a cluster of particles in field h, after saturation, is given by

$$\overline{\cos \varphi(h)} = \int_{0}^{\theta_b} \cos \varphi_1 \sin \theta \, d\theta + \int_{\theta_b}^{90°-\theta_b} \cos \varphi_2 \sin \theta \, d\theta + \int_{90°-\theta_b}^{90°} \cos \varphi_1 \sin \theta \, d\theta. \tag{15}$$

It is dependent only on θ_b, hence, it will also be identical for different pairs a_1, t giving the same a.

From Gaunt's table one can see that for $h < 0$ we have $\Delta\eta\,(45°) = \Delta\eta_{\min}$ and $\Delta\eta(0°) = \Delta\eta(90°) = \Delta\eta_{\max}$ (for $h > 0$ the case is exactly the opposite). To calculate $\Delta\eta$ from Eq. (12) φ_m and φ_1 were found by solving Eq. (11) by the Newton-Raphson iteration method (as $\eta'' \neq 0$ for this problem). The accuracy for cos φ was 10^{-6}. In this way the values for the $\Delta\eta$ (45°) *vs* h (Fig. 3. curve *1*) and $\Delta\eta$ (0°) *vs* h (Fig. 3, curve *2*) curves were computed. Curve *1* is the line for which $t = \tau$ for $\theta = 45°$, whereas curve *2* is the line for which

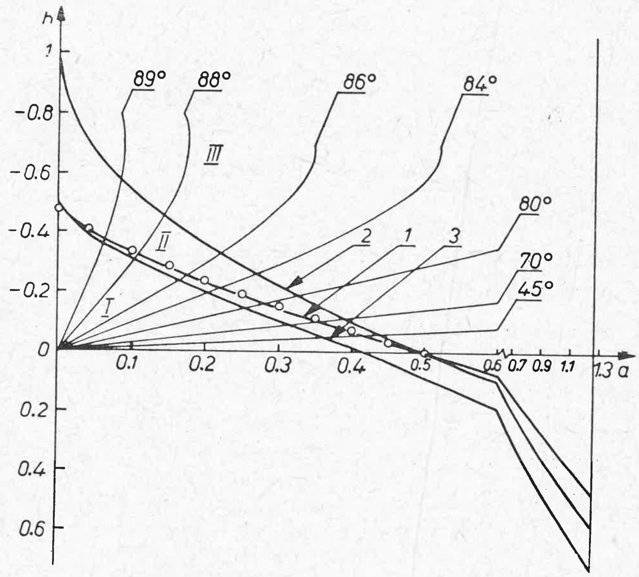

Fig. 3. (h, a) plane for SW particles. I, III are SW behaviour areas, II is the thermal reversal area. Curve *1* is for particles with $\theta = 45°$ and $\tau = t$. Curve *2* is for particles with $\theta = 0°$ and $\tau = t$. Curve *3* is for particles with $\theta = 45°$ and $\tau = 10^2\, t$. The circles represent the coercive force h_c. Curves with indicated values of θ are those for which the population ratio of φ_1 and φ_2 states is exp (−5) for the given θ

$t = \tau$ for $\theta = 0°$. The curve *2* in Fig. 3 can also be calculated analytically from the generalized Bean-Livingston formula (1959): $|h_c| = 1 - \sqrt{2a}$.

For $a < 0.5$ an (h, a) point in Fig. 3 may lie within one of three areas. For a point in area I the component of the magnetic moment along h (previously $h = \infty$) is given by $\int_0^{90°} \cos\varphi_1 \sin\theta d\theta$, what agrees with the values from the top part of the SW hysteresis curve. For a point in area III this component is given by $\int_0^{90°} \cos\varphi_2 \sin\theta d\theta$, *i.e.* by the value from the lower part of the SW hysteresis curve. If the point is in the area II, then when h decreases (h is negative) the groups of particles with $\theta = 45° \pm \alpha$, where α increases from 0° on line *1* to 45° on line *2*, successively fulfil the relation (7) and pass from the φ_1 state to the φ_2 state of lower energy.

For $a > 0.5$ ($h > 0$) the particles represented by an (h, a) point lying below the line *2* begin to decrease the population of the lower minimum φ_1 when the field decreases, to the advantage of minimum φ_2 (this concerns particles with $\theta = 0°$ and 90° for h given by curve *2* up to the particles with $\theta = 45°$ for h given by curve *1*), up to equal populations and zero resulting magnetic moment for $h = 0$.

Demagnetization curves

For $a < 0.5$ ($h < 0$) and given values of a and h, θ_b from Eq. (14) has been calculated (with 0.001° accuracy). The inverse interpolation of $\Delta\eta$ *vs* θ values was found by the use of the inverted Newton formula.

Next, $\overline{\cos\varphi(h)}$ was computed from Eq. (15). First, φ_1 or φ_2 were calculated from Eq. (11) for θ increasing by steps of 3° and also for θ equal to θ_b and $90°-\theta_b$ (the initial values of the solution: φ_1 for $\theta = 0°$ and $90°-\theta_b$ and, φ_2 for $\theta = \theta_b$ were determined graphically). Then the values of the integrand were tabulated in 3° intervals together with the boundary values. Next, the integrand values were interpolated for additional θ's. This enabled us to find the integral in each interval according to the Simpson rule by dividing the interval into two parts: one with the width of the subinterval equal 2°, and the second, very small part, with an automatically chosen width of the subinterval in order to cover θ_b and $90°-\theta_b$. The accuracy was estimated to be 10^{-4}. The results are presented in Fig. 4 by the curves of type I.

For a given a the curves commence from h given by curve *1* in Fig. 3 and terminate on h given by curve *2* in Fig. 3. It is seen that thermal agitation already for $a \geqslant 0.04$ ($K_u V \leqslant 310\, kT$ for $t = 1$ sec) gives distinct shortening of the hysteresis curve which increases with decreasing V (opposite to that for incoherent rotation (Brown 1963)).

Taking into account the general condition for magnetic reversal, instead of the simplified version $t = \tau$, one obtains

$$\cos\varphi(\theta, h) = (1-e^{-t/\tau})\cos\varphi_2 + e^{-t/\tau}\cos\varphi_1 \tag{16}$$

with

$$\tau = \exp[-25(1-\Delta\eta/a_1)]. \tag{17}$$

The reduced magnetization is then expressed by

$$\overline{\cos\varphi(h)} = \int_0^{90°} \cos\varphi(\theta, h)\sin\theta d\theta. \tag{18}$$

In order to compute the integral (18) the values of φ_1, φ_2 and φ_m were tabulated for arbitrary h, with θ varying between 0° and 90° in 3° steps (initial solutions for $\theta = 0°$ were obtained graphically). Subsequently, $\Delta\eta(\theta, h)$ for θ changing every 3° between 0° and 45° were calculated (for larger θ the $\Delta\eta$ are symmetrical with respect to 45°). Having $\Delta\eta$, $\tau(\theta, h)$ were calculated from Eq. (17) and then, using Eq. (16), $\cos\varphi(\theta, h)$ were obtained.

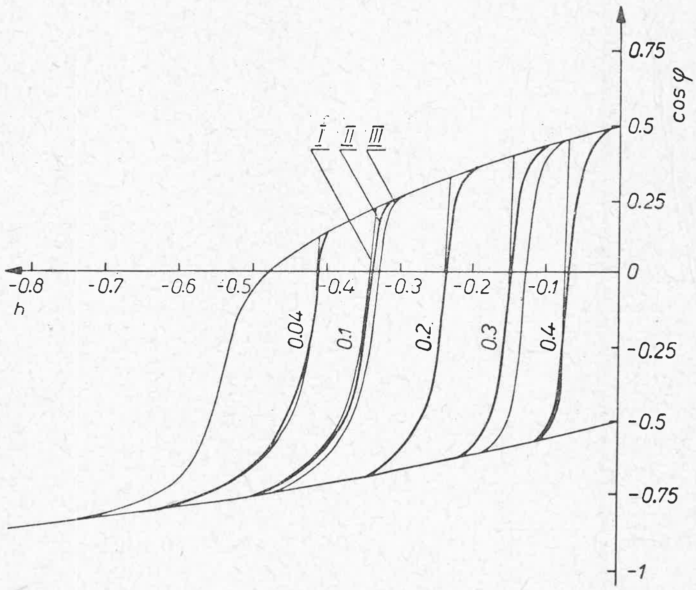

Fig. 4. Demagnetization curves with and without thermal agitation. The values of a (type I) and a_1 (types II, III) are marked in the figure

After tabulating the values of the integrand for θ varying every 3° numerical integration was carried out by the Simpson rule (the largest possible error is one part in 10^4). The obtained $\cos\varphi(h)$ *vs* h curves for $t = 1$ sec and several chosen a_1 are shown in Fig. 4 as curves of type II.

The time intervals during which the individual opposite fields act add together (this means it is impossible to pass to larger h with a remaining constant). Curves of type III in Fig. 5 are an example of demagnetization curves for $a_1 = 0.1$ and 0.3 and for $t = 10$ sec. In reality the hysteresis curve will commence from the curve for $t = 1$ sec, but will end in the region of the curve for $t = 10$ sec.

In Eq. (18), instead of the critical value θ_b, there is an interval $\Delta\theta$ where $\cos\varphi$ varies from $\cos\varphi_1$ to $\cos\varphi_2$ continuously. This interval may be estimated by assuming that t/τ varies with θ between 10^{-4} and 10, what gives

$$\Delta\eta(\theta_1, h) = a' = a[1+4\ln 10/(25+\ln t)] \tag{19}$$

$$\Delta\eta(\theta_2, h) = a'' = a[1-\ln 10/(25+\ln t)] \tag{20}$$

$$\Delta\theta = \theta_2 - \theta_1.$$

From Eqs (19) and (20) one can see that the values of integral (18) will not be identical for various a_1 and t giving the same a (as $\Delta\theta$ will not be identical). Moreover, the demagnetization curves originate not from h corresponding to the intersection of the straight line $a = a^*$ with curve *1* in Fig. 3, but approximately from h determined by the intersection with the $\Delta\eta(45°) = a(1+2 \ln 10/25)$ *versus* h curve (curve *3* in Fig. 3). Curve *3* is the boundary of the areas I and II in Fig. 3.

For increasing t_1 the a' and a'' values approach a and the $\Delta\theta$ effect may be neglected.

The values of coercive force determined from the intersection points of the type II curves (Fig. 4) with the h-axis, are lower than the values obtained for the type I curves. The difference is small and grows from 0 to 0.005 (for a variable from 0 to 0.5). The values of coercive force for curves of type I (determined with an accuracy of 0.001) are plotted in Figs 3 and 6 (circles).

Time variations of magnetic parameters

For the time variations of coercive force it is possible to write in terms of moduli the approximate formula

$$h_c(t) = h_c(a_1) - S(a_1)\,\frac{a_1}{25}\ln t \tag{21}$$

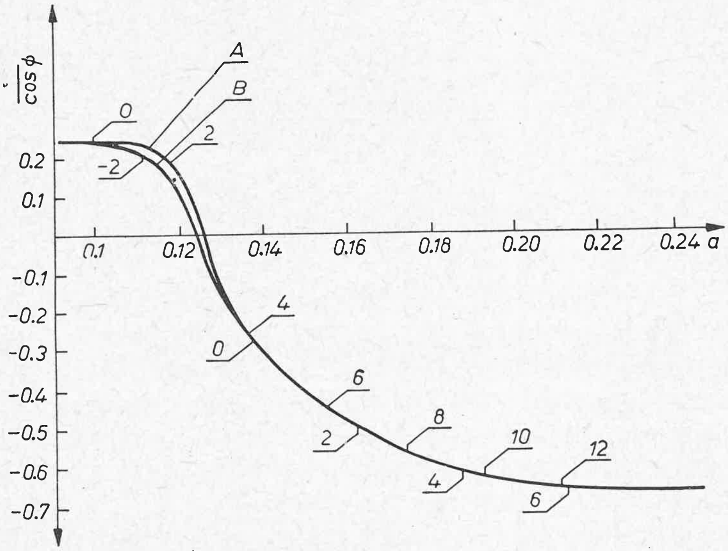

Fig. 5. Magnetization after saturation and application of oppositely directed reduced field $h = -0.31$ as a function of a for $a_1 = 0.1$ (curve *A*) and $a_1 = 0.1368$ (curve *B*). Log$_{10}$ t values are indicated at the curves

where $h_c(a_1)$ is the coercive force when $a = a_1$, *i.e.* for $t = 1$ sec, and $S(a_1) = -(dh_c/da)_{a=a_1}$. If we acknowledge the H_c *vs* a dependence as linear, that is, $h_c = c\,(0.5-a)$ (*cf.* Fig. 6), we get

$$-\frac{dH_c}{d \ln t} \simeq c\,\frac{kT}{VI_S} \overset{\text{def}}{=} S_V$$

S_V is, as shown by Mizia (1969), identical with the constant for the analysis of relaxation along the hysteresis curve introduced by Street (1952).

It is also possible to analyze the time variations of magnetization in this model. The value of a increases logarithmically with time, so that even if the point (h, a_1) is in the region I (Fig. 5) a may reach the curve *3* (Fig. 3) after a certain time. At longer times there will arise a change in magnetization. By way of illustration the magnetization for $h = -0.31$ and $a_1 = 0.1$ (curve A, Fig. 5) and for $a_1 = 0.1368$ (curve B, Fig. 5) were computed from Eq. (18) by substituting an exponentially increasing t. Both curves are drawn as a function of a given by Eq. (14) (values of $\log_{10} t$ are given with the curves). Both curves originate approximately at the intersection of the straight line $h = -0.31$ with curve *3* (Fig. 3) and terminate at the intersection with curve *2* (Fig. 3).

The changes of magnetization are faster for smaller h (as regards absolute value), but for small h the assumption $\tau_{2,1}/\tau_{1,2} \gg 1$ is not satisfied.

Discussion on the $\tau_{2,1}/\tau_{1,2} \gg 1$ assumption

The previous relations were derived with the assumption that the equilibrium state for any very small h is that in which all magnetic moments are in position φ_2. In reality, in the equilibrium state

$$\tau_{1,2}^{-1} n_1 = \tau_{2,1}^{-1} n_2 \tag{22}$$

whence

$$z = \frac{n_2}{n_1} = \frac{\tau_{2,1}}{\tau_{1,2}} = \exp\left(\frac{25}{a_1} \Delta \eta_{1,2}\right) \tag{23}$$

where $\Delta \eta_{1,2} \overset{\text{def}}{=} \eta(\varphi_1) - \eta(\varphi_2)$. z decreases gradually from large values to unity when θ increases from 0° to 90° (for $H<0$). For $\frac{25}{a_1} \Delta \eta_{1,2} = 5$ (the curves with values of θ labelled, Fig. 3) it may be assumed that z^{-1} is approximately equal to zero.

It is seen from Fig. 3 that for small h the ratio of occupation numbers z cannot be neglected for a large group of angles θ and it is then necessary to put into equation (18)

$$\cos \varphi(\theta, h) = \frac{1+z}{z} (1-e^{-t/\tau}) \cos \varphi_2 + (1+z^{-1}) (z^{-1} + e^{-t/\tau}) \cos \varphi_1 \tag{24}$$

and

$$\tau = \frac{1+z}{z} \exp\left[-25 (1-\Delta \eta / a_1)\right]. \tag{25}$$

These expressions are valid for $h > 0$, too.

Analysis of h_c and h_R

Figure 6 depicts the curves of h_c and h_R as a function of a. The data for h_R (reduced remanence coercive force) are taken from the paper by Gaunt (1968). As is seen from the figure, the differences between h_R and h_c for a given a are minute. The difference between

H_R and H_c is evidence of the effective dispersion of the energy barriers in the direction of the measurement. The small difference between h_R and h_c is caused by the fact that the dispersion of the energy barriers due to the isotropic distribution of easy axes is relatively small.

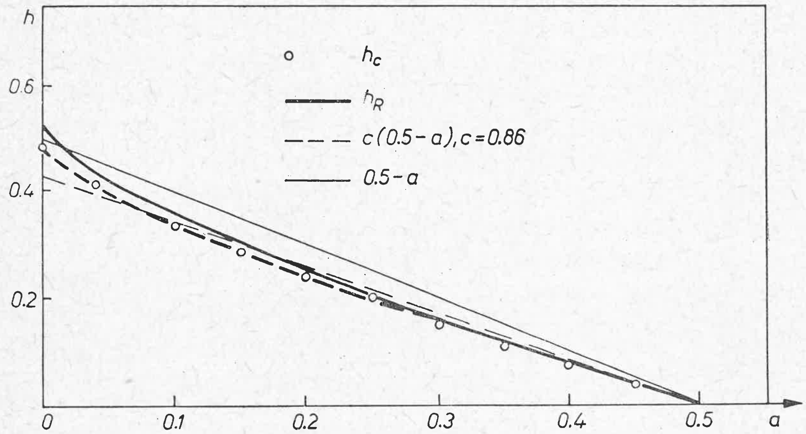

Fig. 6. Reduced fields h_c and h_R, and the straight lines 0.5—a and c(0.5—a) for a chaotic distribution of uniaxial anisotropy axes

In rough approximation h_R and h_c may be assumed to be equal and described by a single straight line, 0.5—a, or to be somewhat more exact, the line c(0.5—a) (Fig. 6). This is equivalent to the statement that the mean spatial energy barrier is given by

$$\bar{E} = K_u V + \frac{1}{c} V I_S H \tag{26}$$

where H has a positive sign for the direction agreeing with that of the saturating field, as had been assumed at the beginning of this paper.

Conclusions

It was shown here that thermal fluctuations give rise to a dependence of the magnetic properties of fine particles on a factor of the form $a = \frac{25\,kT}{2K_u V}\left(1 + \frac{\ln t}{25}\right)$.

The shape of the hysteresis loop and magnetic relaxation of single domain particles under the effect of thermal agitation were found numerically. Shown is the thermal narrowing of the hysteresis loop (Fig. 4) for small volumes, what together with the narrowing due to incoherent rotation for larger volumes causes that the values of coercive force corresponding to the Stoner-Wohlfarth hysteresis loop can never be achieved.

For the coercive force of such a cluster with a chaotic distribution of easy axis the following approximate formula was obtained:

$$H_c = c\,\frac{K_u}{I_S} - c\,\frac{25\,kT}{VI_S}\left(1 + \frac{\ln t}{25}\right), \quad c \approx 0.86.$$

This formula is a generalized version of the Bean-Livingston formula derived for microregions with easy axes aligned parallelly to the magnetic field.

It follows from this formula that $-dH_c/d(\ln t) = c\,\frac{kT}{VI_S} = S_V$, in which, according to Mizia (1969), S_V is the constant for magnetic relaxation introduced by Street (1952).

It was shown that the dispersion of the energy barriers due to the distribution of easy axes is rather small as regards its effect on magnetic observables.

Proof is given that the spatial mean energy barrier of microregions with uniaxial anisotropy and a chaotic distribution of easy axes is approximately described by the linear relation $\overline{E} = K_u V + \frac{1}{c}\,VI_S H$.

A new type of curves for magnetic relaxation is proposed (Fig. 5).

We should like to thank Professor Ludwik Kozłowski for his encouragement and interest in this work.

REFERENCES

Bean, C. P., Livingston, J. D., *J. Appl. Phys.*, **30**, 1209 (1959).
Brown, W. F., *Micromagnetics*, pp, 78–80, J. Wiley & Sons, New York 1963.
Gaunt, P., *Phil. Mag.*, **17**, 265 (1968).
Mizia, J., *Doctor's thesis* (1969).
Néel, M. L., *C. R. Acad. Sci.* (Paris), **228**, 664 (1949).
Oquey, M. J., *Proc. IRE*, **48**, 1165 (1960).
Street, R., Woolley, J. C., Smith, P. B., *Proc. Phys. Soc.* (London), **B65**, 679 (1952).
Stoner, E. C., Wohlfarth, E. P., *Phil. Trans. Roy. Soc.*, **A240**, 589 (1948).